Jansen JD (2006). Flood magnitude-frequency and lithologic controls on bedrock river incision in post-orogenic terrain. Geomorphology, 82, 39–57. doi: 10.1016/j.geomorph.2005.08.018

Flood magnitude–frequency and lithologic control on bedrock river incision in post-orogenic terrain

John D. Jansen

Department of Geographical and Earth Sciences, University of Glasgow, G12 8QQ, Scotland

Abstract

Mixed bedrock–alluvial rivers–bedrock channels lined with a discontinuous alluvial cover–are key agents in the shaping of mountain belt topography by bedrock fluvial incision. Whereas much research focuses upon the erosional dynamics of such rivers in the context of rapidly uplifting orogenic landscapes, the present study investigates river incision processes in a post-orogenic (cratonic) landscape undergoing extremely low rates of incision (<5 m/Ma). River incision processes are examined as a function of substrate lithology and the magnitude and frequency of formative flows along Sandy Creek gorge, a mixed bedrock–alluvial stream in arid SE-central Australia. Incision is focused along a bedrock channel with a partial alluvial cover arranged into riffle-pool macrobedforms that reflect interactions between rock structure and large-flood hydraulics. Variations in channel width and gradient determine longitudinal trends in mean shear stress (τ_b) and therefore also patterns of sediment transport and deposition. A steep and narrow, non-propagating knickzone (with 5% alluvial cover) coincides with a resistant quartzite unit that subdivides the gorge into three reaches according to different rock erodibility and channel morphology. The three reaches also separate distinct erosional styles: bedrock plucking (i.e. detachment-limited erosion) prevails along the knickzone, whereas along the upper and lower gorge rock incision is dependent upon large formative floods exceeding critical erosion thresholds (τ_c) for coarse boulder deposits that line 70% of the channel thalweg (i.e. transport-limited erosion).

The mobility of coarse bed materials (up to 2 m diameter) during late Holocene palaeofloods of known magnitude and age is evaluated using step-backwater flow modelling in conjunction with two selective entrainment equations. A new approach for quantifying the formative flood magnitude in mixed bedrock–alluvial rivers is described here based on the mobility of a key coarse fraction of the bed materials; in this case the d_{84} size fraction. A 350 m^3/s formative flood fully mobilises the coarse alluvial cover with τ_b~200–300 N/m^2 across the upper and lower gorge riffles, peaking over 500 N/m^2 in the knickzone. Such floods have an annual exceedance probability much less than 10^{-2} and possibly as low as 10^{-3}. The role of coarse alluvial cover in the gorge is discussed at two scales: (1) modulation of bedrock exposure at the reach-scale, coupled with adjustment to channel width and gradient, accommodates uniform incision across rocks of different erodibility in steady-state fashion; and (2) at the sub-reach scale where coarse boulder deposits (corresponding to τ_b minima) cap topographic convexities in the rock floor, thereby restricting bedrock incision to rare large floods.

While recent studies postulate that decreasing uplift rates during post-orogenic topographic decay might drive a shift to transport-limited conditions in river networks, observations here and elsewhere in post-orogenic settings suggest, to the contrary, that extremely low erosion rates are maintained with substantial bedrock channel exposure. Although bed material mobility is known to be rate-limiting for bedrock river incision under low sediment flux conditions, exactly how a partial alluvial cover might be spatially distributed to either optimise or impede the rate of bedrock incision is open to speculation. Observations here suggest

that the small volume of very stable bed materials lining Sandy Creek gorge is distributed so as to minimise the rate of bedrock fluvial incision over time.

Keywords: Arid; Craton; Detachment-limited; Palaeoflood; Riffle-pool; Steady state; Transport-limited

1. Introduction

Rivers incise bedrock when the mean shear stress exceeds a critical threshold to initiate erosion. Where the channel is partially lined with coarse debris, as with mixed bedrock–alluvial streams, the bed materials must be entrained before bedrock incision can take place (Gilbert, 1877; Seidl and Dietrich, 1992). Wolman and Miller (1960) observe that the frequency of geomorphically effective events is inversely proportional to the threshold of erosion. Given the high threshold conditions that characterise mixed bedrock–alluvial rivers, sediment transport and bedrock erosion is typically episodic and restricted to infrequent, high magnitude floods (Tinkler, 1971; Baker, 1977; Howard, 1987).

Recognition of coupling and feedbacks between tectonics, climate and geomorphic processes has focused much attention on bedrock rivers and their role in hillslope erosion, regional denudation and sediment flux to basins (e.g. Molnar and England, 1990; Beaumont et al., 1992; Raymo and Ruddiman, 1992; Small and Anderson, 1995; Willet, 1999; Whipple and Tucker, 1999; Hovius, 2000). The push to understand evolution of topography in response to tectonic and climatic forcing has been led with some success by bedrock fluvial incision models that relate incision to the mean shear stress (or stream power) exerted by the formative discharge, with the general form:

$$E = KA^m S^n \quad (1)$$

where E is bedrock river incision rate, K is a dimensional erosion coefficient, A is drainage area (a proxy for discharge), S is channel gradient, and m and n are positive constants. Yet, much debate continues over the ability of K, m, and n to account for aspects of sediment flux, substrate erodibility, and channel width (e.g. Howard and Kerby, 1983; Sklar and Dietrich, 1998; Stock and Montgomery, 1999; Whipple and Tucker, 1999; Sklar and Dietrich, 2001; Whipple and Tucker, 2002). Such surface process models (SPMs) often assume that flow competence during floods exceeds the critical threshold for erosion of bedrock, or overlying coarse debris, and so the threshold term may be neglected. However, erosion thresholds are now demonstrated to be a significant impediment to bedrock incision, and recent emphasis on the importance of mobility thresholds has extended to the level of individual floods within a stochastic distribution, or flow regime (e.g. Tucker and Bras, 2000; Baldwin et al., 2003; Snyder et al., 2003; Tucker, 2004). The crude representation of flow regime in most SPMs, and the sensitivity of these to erosion thresholds and sediment transport processes, more generally, calls for field studies documenting the magnitude and frequency of formative floods in a range of climatic and tectonic settings.

This paper assesses bedrock river incision along an arid zone gorge in cratonic central Australia. Fluvial incision along this mixed bedrock–alluvial river is extremely slow due to the minimal geomorphic activity typical of dry, low relief cratons. Field measurements of channel morphology and bed materials are used to infer responses to large formative floods known from a previous sedimentologic study of late Holocene palaeofloods (Jansen and Brierley, 2004). Long-term incision is found to depend upon the magnitude and frequency of large floods competent to mobilise coarse bed materials that otherwise shield the underlying bedrock from erosion. Lithologic controls on channel morphology and therefore the spatial variation in mean shear stress are shown to dictate reach-scale and channel-scale erosional style and, consistent with slow rates of bedrock incision, formative floods are estimated to have an annual exceedance probability much less than 10^{-2} and possibly as low as 10^{-3}.

2. Bedrock incision styles in mixed bedrock–alluvial channels

River bed-materials play a fundamental role in channel evolution; their size attributes and spatial distribution exert primary control on incision, sediment transport rate and long profile development (Howard, 1980, 1987; Seidl and Dietrich, 1992; Howard et al., 1994; Sklar and Dietrich, 1998, 2001; Gasparini et al., 2004). It is widely assumed that channel gradient along alluvial channels is set primarily by sediment flux, but as channels steepen and bed materials coarsen, critical thresholds of mobility relating to a coarse but minor fraction of the total load come to exert the principal

control (Howard, 1980; Prestegaard, 1983; Hey and Thorne, 1986; Howard, 1987). Erosion of bedrock underlying these 'coarse-bed threshold' channels may occur at high stage, even though a coherent alluvial cover exists during low flows (Howard and Kerby, 1983). In this case, bedrock incision depends upon sediment transport capacity and is therefore transport-limited. Excess sediment transport capacity relative to sediment supply results in exposed bedrock reaches in which channel gradient and incision depend upon the capacity of the flow to detach bedrock: a detachment-limited condition (Howard, 1980; Whipple and Tucker, 1999). Channel processes that contribute to bedrock incision are plucking, abrasion (by both bed load and suspended load), solution, and cavitation. Lithology is a strong determinant of which of these is dominant (Baker, 1988; Miller, 1991; Hancock et al., 1998; Wende, 1999). Whipple et al. (2000) contend that plucking is the rate-limiting style of erosion in rocks that are well-jointed at the sub-metre scale, whereas abrasional processes dominate in massive, unjointed rocks or those with wide joint spacings relative to the magnitude of mean shear stress. The rate of bedrock erosion by plucking is thought to be roughly linear with shear stress beyond a critical threshold (Whipple et al., 2000; Snyder et al., 2003), though rock dip and strike relative to flow orientation also influence plucking efficiency (Miller, 1991; Wende, 1999). Owing to the difficulty in accounting for the suite of processes involved, no quantitative mechanistic model of bedrock erosion by plucking exists (Whipple et al., 2000).

The effect on fluvial incision of non-linearity between mobility of coarse bed materials and discharge is complicated by downstream variations in mean shear stress. Such variations commonly arise where rivers incise rocks of differing erodibility, and the resultant variable channel width and/or gradient affect flow competence and therefore spatial patterns in sediment transport and deposition along the channel. Several studies document close accordance between rock structure, large flood hydraulics and macrobedforms such as riffle-pool morphology along mixed bedrock–alluvial channels (e.g. O'Connor et al., 1986; Baker, 1988; Wohl, 1992a,b). It seems plausible that the same spatial patterns of mean shear stress and energy expenditure also drive bedrock incision along such rivers (Wohl et al., 1994, Wohl and Merritt, 2001).

3. Field area

Sandy Creek is a 4th-order stream draining 44 km^2 of the NE flank of the Barrier Range (31°00′S, 141°45′E), 100 km NNE of Broken Hill in SE central Australia (Fig. 1). The regional climate is arid, with median annual rainfall of 231 mm ($1\sigma = 118$ mm) at nearby Fowlers Gap (1966–1996), and pan evaporation ~2800 mm/a (Bureau of Meteorology, 1988). Just a few days of streamflow occur per year. Flow gauge data from an adjoining 20 km^2 catchment, Homestead Creek, reveal an extreme index of flow variability of 0.92 (i.e. the standard deviation of the logarithms of the annual flood peaks), which is probably representative of streams in the region.

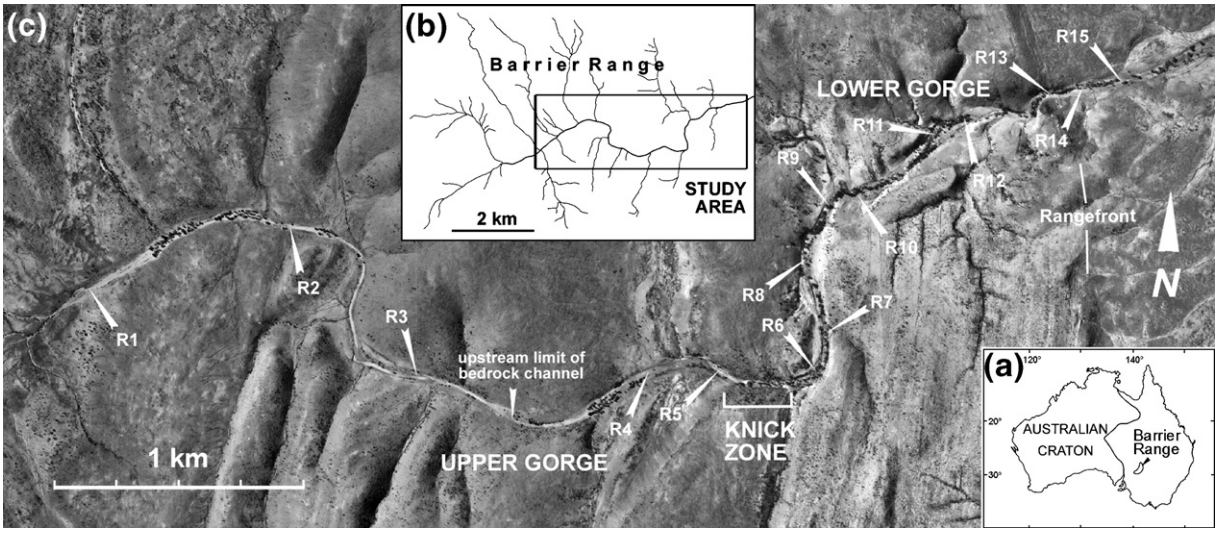

Fig. 1. (a) Field area location in SE-central Australia: the Barrier Range is an outlier of the Australian Craton. (b) Positioning within the Sandy Creek catchment. (c) Reaches and riffle (R) sites: R1–R15. The Devonian strata strike approximately N–S and flow is W to E.

3.1. Geologic setting

Most of the Australian continental interior is of the 'shield and platform' morphostructural type consisting of cratonic basement rocks sporadically exposed above near-horizontal cover rocks. The Australian Craton (Fig. 1a) has remained practically free of major tectonism since the Proterozoic, though broad epeirogenic movements during the Cenozoic have influenced drainage evolution (Veevers, 1984; Gale, 1992; Hill et al., 2003). The Barrier Range traces the eroded stump of a Proterozoic orogenic belt, a cratonic outlier, which has undergone continuous subaerial denudation throughout the Cenozoic (Veevers, 1984). A hint of its once substantial relief is given by K–Ar ages (~500 Ma) on clastic grains found within the Early Jurassic Surat Basin (1000 km to the east), which coincide with a phase of retrogressive metamorphism in the Barrier's Proterozoic basement rocks (Martin, 1981). These fault-bounded uplands are shaped by a combination of faulting and erosional resistance with outlines of relief and drainage reflecting structural trends in the Devonian strata and Proterozoic basement (Mabbutt, 1973; Gibson, 2000). Sandy Creek gorge cuts transverse to this structure with gently dipping Devonian Nundooka sandstones–mostly fine-grained quartzose arenites–forming broad cuestas that stand 100–200 m above the flanking piedmont and plains (Fig. 1c). Resistant silica-cemented arenites (quartzites) form the axes of cuesta ridges, which intersperse wide tributary strike-valleys cut in relatively weak, kaolinite-cemented arenites (Ward et al., 1969; Neef et al., 1995). The gorge has incised below local duricrusted residuals (of probable Late Eocene age) at a rate of ~0.9–4.7 m/Ma (Jansen, 2001), which is comparable with rates elsewhere on the craton, such as the Yilgarn Block (~0.5 m/Ma; van de Graaf, 1981), the Kimberley Block (~0.7 m/Ma; Wilford, 1991), and the Eyre Peninsula (~0.7 m/Ma; Bierman and Turner, 1995). Gorge incision is probably a response to base level fall caused by monoclinal flexure at the rangefront due to ?Neogene thrusting at depth along the fault-bound NE flank of the ranges, though vertical displacement was probably less than 50 m in total (Gibson, 2000; Jansen, 2001).

3.2. Reach and channel morphology

The 4 km main stem length of the gorge is incised mostly transverse to the strike of the Devonian strata, these strata dip 10–25° in a downstream direction steepening to 39° close to the rangefront monocline. A massive quartzite unit (55 m thick) marks a 260 m length of steep, confined bedrock channel termed the knickzone, which splits the gorge into three reaches reflecting contrasts in rock erodibility (Figs. 1c and 2). The term 'knickzone' is used here to mean a relatively steep section of channel separating reaches of lower gradient irrespective of whether produced by tectonic deformation, base level fall or variable rock resistance.

Rock incision is focused along a bedrock channel that extends upstream to a point indicated in Fig. 1c. Reaches further upstream contain negligible bedrock outcrop (~1%), and are not actively incising. A 2–3 m high strath terrace is preserved discontinuously along the upper and lower gorge reaches, but is absent along the knickzone where the channel occupies the full width of the gorge. Channel width is highly variable downstream, with most constrictions attributable to quartzite outcrops (Fig. 2). Although separated by the clearly narrower and steeper knickzone, the upper and

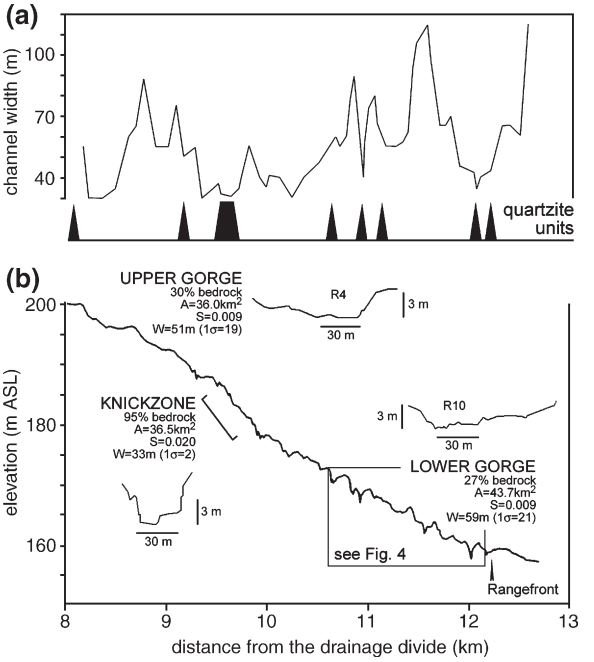

Fig. 2. (a) Downstream relations between bedrock channel width, lithology and channel gradient. The position and extent of quartzite units within the Devonian strata (indicated by the width of the black triangles) correspond to major constrictions. (b) Longitudinal bed profile and representative cross-sections for the upper gorge (R4), knickzone, and lower gorge (R10) (see Fig. 1c for sites). Drainage areas (A) were calculated at the reach's downstream limit; reach-averaged channel gradients (S) were determined by linear regression of the thalweg profile data; reach mean channel widths (W) were determined from measurements orthogonal to the channel at 100 m intervals. Percentage bedrock refers to the proportion of the channel thalweg floored with exposed bedrock. Mean channel gradient declines to 0.004 beyond the rangefront.

lower gorge reaches have equivalent mean channel gradient and mean bedrock channel width (within 1σ error). The significance of this arrangement is discussed later.

Minimal sediment storage along the knickzone permits detachment-limited bedrock erosion wherein coarse, joint-defined tabular blocks are plucked and stacked in imbricated clusters nearby (Fig. 3a,b; Brayshaw, 1984; Wende, 1999). Bed load impacts and hydraulic wedging–processes that drive joint crack propagation–probably contribute by preconditioning the rock for plucking (Hancock et al., 1998; Whipple et al., 2000). Evidence of abrasion by bed load and suspended load, such as potholes and fluting, occurs locally on both the weaker kaolinite-cemented arenites and resistant quartzites, but is probably of secondary importance because abraded blocks are ultimately plucked from joints. An extensive (95%) bedrock outcrop along the knickzone includes numerous successive upstream-facing (positive) steps spanning the channel, each marking the removal of joint blocks (Fig. 3a). The height and spacing of individual steps is a function of the dip and spacing of joint sets. Horizontal joints are spaced fairly regularly at ~1 m intervals, with vertical joints spaced at ~1–3 m (Fig. 3a). Bedrock plucking proceeds down-dip along joint planes progressively incising bedrock in a downstream direction. Thus with ongoing gorge incision the knickzone migrates extremely slowly *downstream* following the regional dip—yet such knickzones are regarded as non-propagating, as opposed to incisional waves that propagate upstream from a point of base level fall.

Transport-limited conditions prevail in the upper and lower gorge due to the semi-continuous cover of coarse fluvial deposits, which covers 70% and 73% of the channel thalweg, respectively (Fig. 3c). This coarse alluvial cover is organised into riffle-pool macrobedforms up to 2 m in thickness (Fig. 4a,b). The lower gorge, in particular, contains well-defined riffle-pool morphology that closely reflects rock control on channel width variability downstream. Pools with inset fills are located at constricted channel bends (~35–45 m wide) associated with thin quartzite units (1–5 m thick). These intersperse coarse boulder riffles along gorge expansions (~80–100 m wide), which as will be shown later correspond to flow competence minima during large floods (Fig. 4c). The pool constrictions function as a series of nozzles during rare large floods in which the pools are flushed of stored sediment (Kieffer, 1985). The riffles resemble expansion bars (Baker, 1978, 1984), and are the major coarse-sediment storage units in the gorge. Riffle crests typically consist of a pile of 1 to 3 clast-supported boulders with fine interstitial sediments. As shown in Figs. 2 and 4b, many riffles form pronounced topographic highs above pool

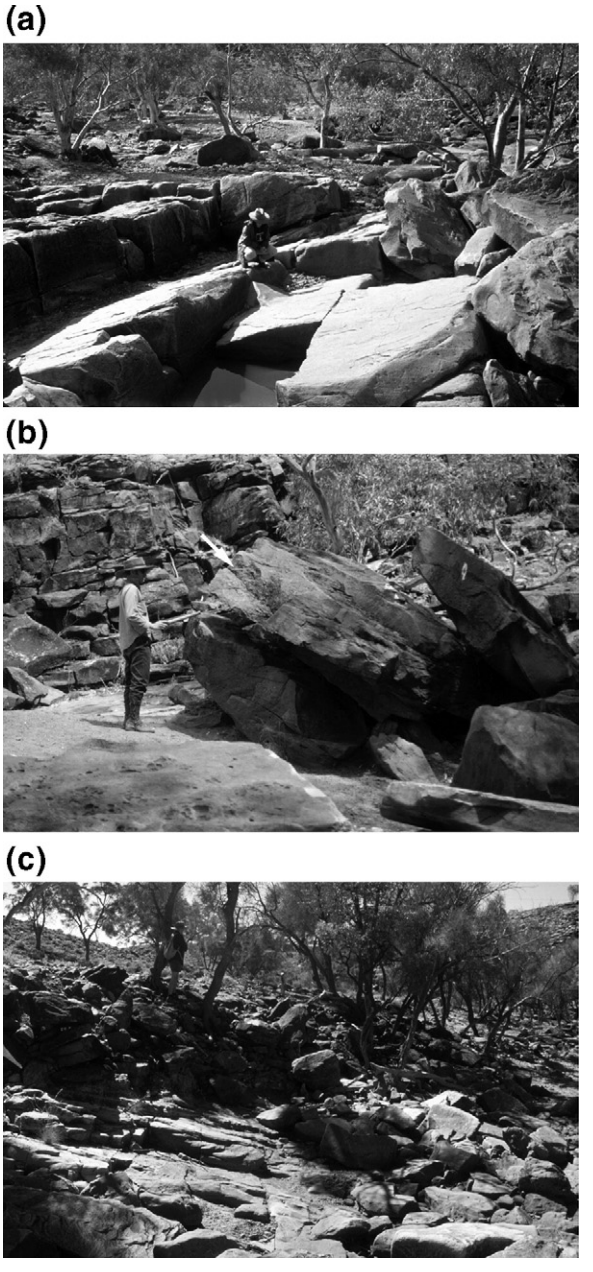

Fig. 3. (a) View downstream of the knickzone with exposed joints dipping ~11–13° and spaced 1–3 m; note large imbricated blocks downstream stacked against positive bedrock steps (trees grow subsequently in the protected lee of these bedforms). (b) Imbricated slabs plucked from nearby exposed bedrock joints; the arrow indicates a block measuring 4700×3200×1200 mm (flow from right to left). (c) Boulder mantle and a segment of exposed bedrock in the lower gorge, near R6, where kaolinite-cemented arenites have joints spaced 0.1–0.4 m.

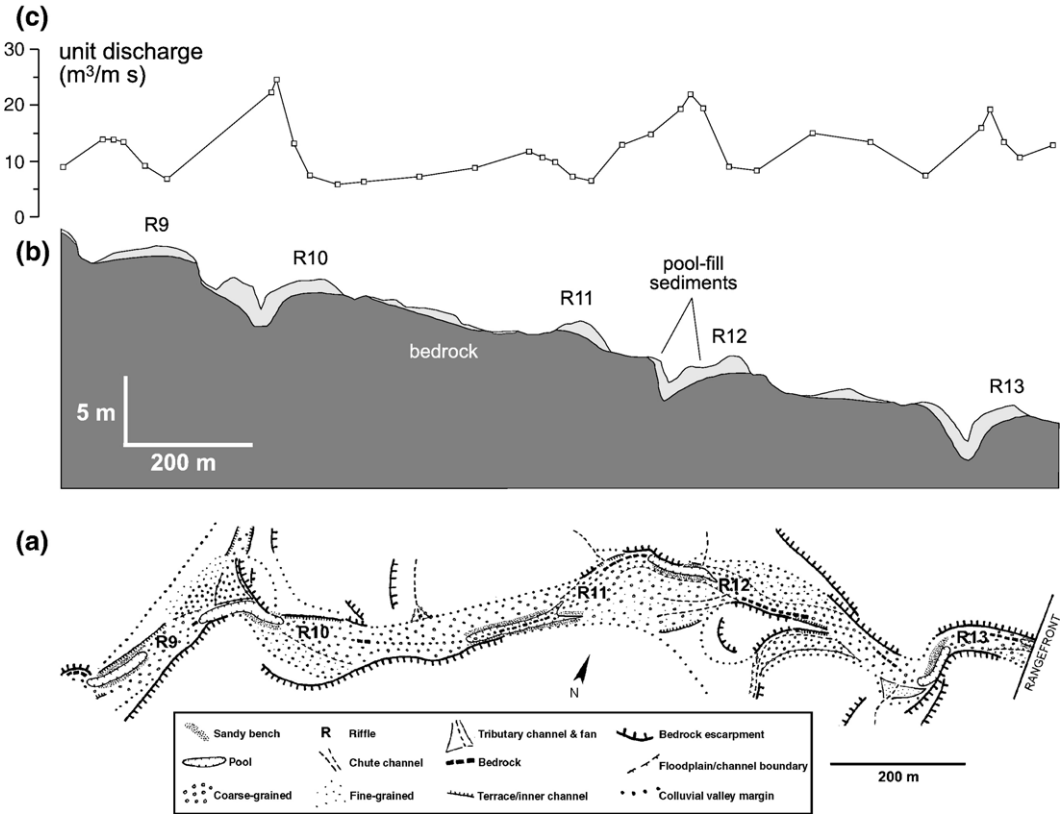

Fig. 4. Detail of morphology and flow competence in part of the lower gorge. (a) Planform map of valley floor morphology (flow from left to right), with riffles (R) listed in Table 1. (b) Long profile, indicated in (a), showing undulating riffle-pool morphology with convexities in the rock floor capped by boulder riffles that grade to mainly fine-sediment pool-fills (light-shading) in the intervening notches. (c) Downstream variation in discharge per unit width (HEC-RAS unit discharge outputs for the 350 m^3/s flood, Q_{p2}). Riffles correspond to flow competence minima during large floods, whereas flow convergence caused by resistant quartzite outcrops at the pools concentrates scour and leads to episodic flushing of pool-fills (Jansen and Brierley, 2004).

'notches' in the bed profile. The coarsest unit on major riffles forms a lobe extending along the thalweg from the pool-tail to the riffle crest. The largest boulders on the riffle crests are up to 2 m (*b*-axis) and these usually grade laterally onto a narrow, coarse-grained floodplain. A 1965 photograph of R10 shows that large boulders on the riffle crest have remained stationary over the subsequent 40-year period. This infrequency of bed material mobility is key to transport-limited bedrock incision in the upper and lower gorge.

4. Bed materials size attributes

The grain size of channel bed materials at-a-site and downstream is a function of sediment supply and sediment transport processes: abrasion and hydraulic sorting. Sediment may be supplied to the channel from bedrock outcrops, slopes, tributary inputs, and reworking of stored sediments. In Sandy Creek gorge, plucking from exposed bedrock joints supplies the coarsest bed materials and is therefore most relevant to flow competence analyses here.

Abrasion and hydraulic sorting inevitably co-exist in coarse-bed streams. Bed materials are progressively reduced in size by abrasion while floods selectively entrain certain fractions thereby determining their distribution along the channel (Rana et al., 1973; Schumm and Stevens, 1973; Knighton, 1998). Sternberg (1875) proposed an exponential relationship to describe downstream-fining due to abrasion, though it describes the results of selective entrainment equally well (e.g. Church and Kellerhals, 1978; Troutman, 1980):

$$w = w_0 e^{-\alpha L} \quad (2)$$

where w=particle weight at L, the distance travelled; w_0=initial particle weight; α=coefficient for effects of

abrasion and sorting. According to this function, the rate of downstream fining (α) is fastest among coarse fractions and decreases with smaller sizes. However, interactions between sediment supply and sediment transport processes are complicated in mixed bedrock–alluvial channels, because the close proximity to sources of coarse sediment and abrupt variations in valley confinement and gradient tends not to produce simple decline in clast size downstream (e.g. Hack, 1957; Miller, 1958; Knighton, 1980; Rhoads, 1989; Rice, 1998). Understanding the relative influence of these factors is necessary before clast size data can be used reliably in flow competence analyses.

4.1. Clast size analysis: methods and results

Clast size characteristics of the riffle coarse locales were determined by measuring 100 clasts at each riffle using a modified version of the Wolman (1954) method for measuring bed surface gravels (Brierley and Hickin, 1985). The riffles have neither log-normal nor other ideal clast size distributions, but rather complex bimodal or polymodal distributions (Fig. 5b, Table 1—see table footnotes for definitions of d_{5x} and d_x). Longitudinal clast size trends for selected percentiles indicate downstream-coarsening above the knickzone; whereas below, coarser fractions show slight downstream-fining and finer fractions show no overall trend (Fig. 5a). The trends downstream of the upper gorge are the focus here. The coarse fraction peaks (d_{84}, d_{95}, d_{5x}) shown in Fig. 5a correspond to riffles immediately downstream of quartzite outcrops that form the most constricted sections; the coarsest blocks commonly rest within a few tens of metres of their bedrock source. Size sorting is poor on the riffles (coefficient of variation, $C_v \sim 1$) and, consistent with steep rocky channels elsewhere, there is no evidence for improved sorting downstream (e.g. Miller, 1958; Inderbitzen, 1959).

The combined clast size dataset ($n = 1500$) is unimodal. Cumulative frequency curves were used to discriminate modes within each riffle population; these occur as steepening or segmentation in the curves (see

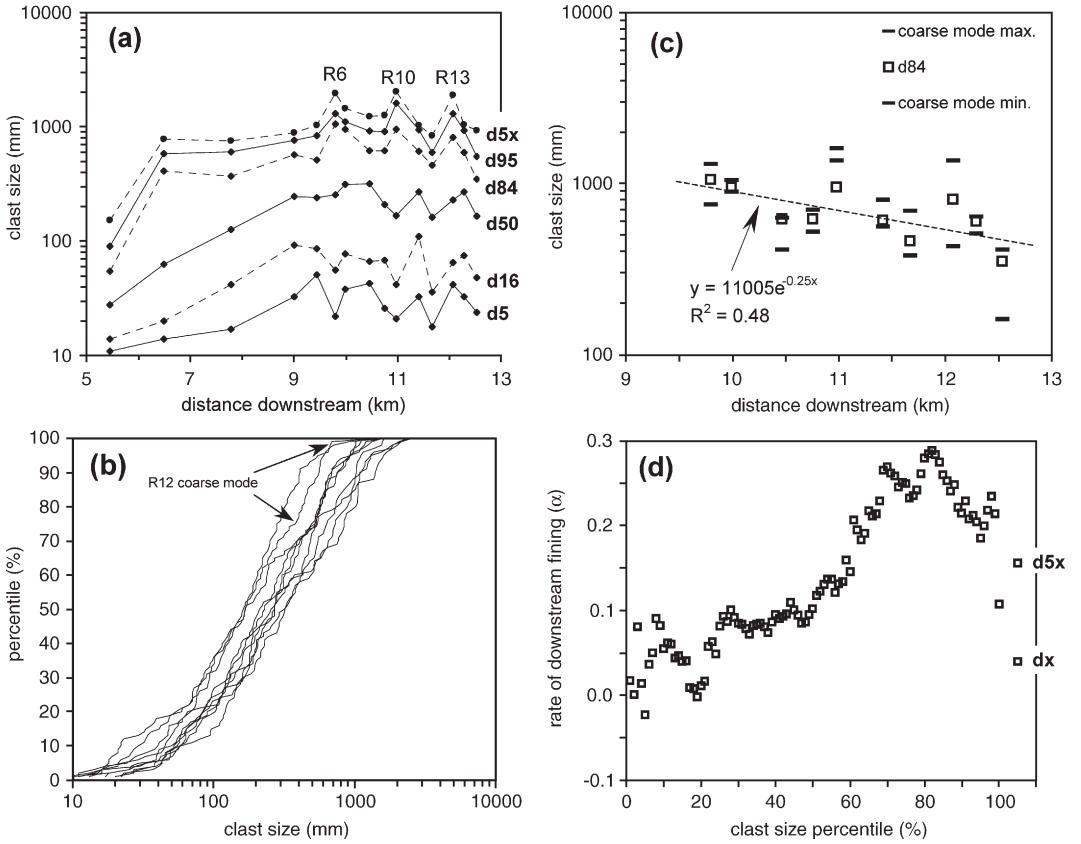

Fig. 5. (a) Clast size trends downstream with the coarsest riffles: R6, 10 and 13, marked. (b) Clast size cumulative frequency curves for R6–R15, including the example of the R12 coarse mode. (c) Size range of the coarse mode at riffles R6–R15, fitted with the d_{84} exponential regression. (d) The rate of downstream fining (α) for each of the clast size percentiles R6–R15 (d_{5x} and d_x are included).

Table 1
Summary of clast-size attributes at each riffle

Riffle	Distance downstream (km)[a]	d_5	d_{16}	d_{50}	d_{84}	d_{95}	d_{5x}[b]	d_x[c]	Mean	C_v[d]	Lithology (% sandstone)	Modality[e]
R1	5.445	11	14	28	55	90	152	242	39	0.91	36	Strongly unimodal
R2	6.492	14	20	63	410	580	782	697	174	1.21	59	Strongly bimodal
R3	7.786	17	42	127	370	605	755	745	206	0.96	90	Strongly unimodal
R4	9.075	33	93	245	570	760	882	721	313	0.75	96	Unimodal
R5	9.445	51	86	240	515	840	1034	1166	303	0.85	91	Unimodal
R6	9.797	22	56	255	1050	1300	1960	2300	502	1.04	45	?Trimodal
R7	9.993	38	78	315	950	1100	1451	1700	463	0.87	67	Weakly bimodal
R8	10.464	43	67	318	620	920	1227	1449	379	0.81	68	Strongly bimodal
R9	10.752	26	68	210	620	910	1256	1616	332	0.94	96	Weakly bimodal
R10	10.975	21	42	168	950	1600	2016	1715	428	1.30	77	Weakly bimodal
R11	11.410	33	110	270	610	940	1026	1249	342	0.77	86	Unimodal
R12	11.667	18	36	162	460	600	840	1645	239	0.97	75	Polymodal
R13	12.072	42	65	230	810	1300	1892	1722	445	1.07	98	Strongly bimodal
R14	12.289	33	75	270	600	930	1048	1196	337	0.83	77	Weakly bimodal
R15	12.533	24	48	166	350	550	924	1970	220	1.02	71	?Weakly bimodal
Total data	_	20	46	200	600	1020	2332	2300	324	1.09		Unimodal

All clast sizes are intermediate axes (*b*-axes) measured in mm. Percentiles d_5, d_{16}, d_{50}, d_{84}, d_{95}, d_{5x} represent the overall population characteristics.
[a] Distance from the drainage divide.
[b] d_{5x} is the arithmetic mean of the *b*-axes measured from the five largest clasts surveyed on each riffle, as distinct from the five largest boulders present, and thus reflects the entire population sample of 100 clasts at each riffle.
[c] d_x is the cubed root of the product of the *a*-, *b*- and *c*-axes measured from the largest clast on each riffle.
[d] Coefficient of variation (C_v) equals the standard deviation divided by the arithmetic mean.
[e] Modality is assessed qualitatively from the cumulative frequency plots.

example, Fig. 5b), and bimodal or polymodal distributions contain discrete subpopulations. As with size trends, the knickzone separates differing modality characteristics along the gorge. Unimodality prevails upstream and the unimodal class range coarsens consistent with the size trend shown in Fig. 5a. Modality downstream of the knickzone is more complex. Immediately downstream of R6, a very coarse mode comprising medium to large boulders (750–1300 mm) emerges and persists on riffles downstream. The coarse modes generally span d_{75}–d_{95} and when plotted in terms of clast size they are well represented by the d_{84} exponential regression curve (Fig. 5c).

The highest percentiles (d_{5x}) reflect large blocks plucked from exposed joints. Such blocks are essentially immobile with no tendency for downstream fining (Fig. 5a). It is postulated that the coarsest of those boulders that are still influenced by selective entrainment will show the fastest rate of downstream fining consistent with Sternberg's function (Eq. (2)). Fig. 5d presents the rate of downstream fining (α) in the lower gorge for each of the 100 clast size percentiles: the rate of fining is fastest over the range $\sim d_{68}$–d_{88}. Erosional thresholds associated with these coarse mode boulders are key to their role in shielding the underlying rock floor. Flood magnitudes associated with mobility threshold conditions are estimated in the following sections.

5. Flow competence and bed material mobility

The flow competence of palaeofloods is widely inferred from their coarse-grained deposits (e.g. Costa, 1983; Williams, 1983; Baker and Pickup, 1987; Wohl, 1992a). Palaeohydrologic applications are dependent upon progressive entrainment of finer to coarser particles over some measurably wide range of flow conditions. Equal mobility, wherein particles of all sizes move at roughly the same mean shear stress due to particle shielding effects (Parker et al., 1982), might apply at high excess shear stresses and transport rates; however, some degree of size selection certainly occurs at shear stresses up to about twice the threshold of motion (Ashworth and Ferguson, 1989; Parker, 1990), and this is consistent with conditions in Sandy Creek gorge.

On a bed of mixed particle sizes flow competence is a function of clast-size relative to the surrounding population (Komar, 1987; Parker, 1990; Ferguson, 1994; Komar, 1996). Thus, selective entrainment equations that incorporate some measure of the ambient size population have a stronger physical basis compared to those that do not. Mean boundary shear stress, the amount of drag exerted per unit area of the channel bed, is used widely in flow competence analyses via some form of the Shields (1936) criterion. One such approach applicable to poorly sorted gravel is that of

Komar (1987), which estimates the critical shear stress (τ_c) for a given clast relative to the median diameter of the deposit as a whole:

$$\tau_c = 0.045(\rho_s - \rho)g d_{50}^{0.6} d^{0.4} \quad (3)$$

where ρ_s is the density of clasts (2650 kg/m^3), ρ is the density of water (1000 kg/m^3), g is gravitational acceleration, and d is clast diameter. Based on Schoklitsch (1962), Bathurst and colleagues (Bathurst et al., 1983, 1987; Bathurst, 1987) derive an alternative approach using discharge per unit flow width, or critical unit discharge (q_c). Bathurst's original equations are reworked by Ferguson (1994) and the modified formulation is used here:

$$q_c = a\, d_{50}^{1.5} (d/d_{50})^{(1-x)(c+1.5)} / S^{c+1} \quad (4)$$

$$a = m(8g)^{0.5}((\rho_s/\rho - 1)\tau_c{}^*{}_{50})^{c+1.5} \quad (5)$$

where x is the hiding factor (x=0.90; Parker, 1990), c and m are constants relating to the chosen flow resistance relationship (c=0.37, m=1.14; Thompson and Campbell, 1979), and $\tau_c{}^*{}_{50}$ is the critical dimensionless shear stress to entrain the median clast size ($\tau_c{}^*{}_{50}$=0.045).

The critical-stress approach and critical-discharge approach are both sensitive to factors that are difficult to quantify in the field (Ferguson, 1994). Both are strongly influenced by the choice of critical dimensionless shear stress and, whereas discharge is easier to define than shear stress under turbulent conditions, the critical-discharge approach is sensitive to the chosen hiding factor and flow resistance law. In order to evaluate the mobility of the riffle boulders, the two selective entrainment approaches are used in conjunction with field-based discharge estimates from field observations and flow modelling.

5.1. The 1992 flood

A high magnitude rainstorm on the 18th December 1992 caused major regional flooding. Over the days that followed, a detailed field assessment was conducted in Sandy Creek. Cross-sections measured pre-flood and post-flood indicated minor change along the lower gorge: pool-fill bench surfaces were scoured by 10–20 mm, small gravels were deposited on coarse-grained floodplains, and some minor gullying was evident on terrace margins. Gravel transport was evaluated via a number of pre-flood and post-flood photographs; examples are summarised in Table 2. According to the post-flood field assessment, cobble-sizes were generally mobile with localised transport of small boulders. When compared with clast size percentiles on nearby (upstream) riffles, the mobile clasts correspond to d_{50}–d_{60} with some isolated boulders up to d_{77}.

Table 2
Observed sediment transport following the 1992 flood

Site	Clast sizes transported	Equivalent percentile on nearby riffle
P2	Mostly cobbles ~200 mm	d_{72}
	One boulder 456×392×90 mm	d_{74}
R2	Transport/exposure of cobbles	d_{72}
R4	Mostly cobbles ≤250 mm	$\leq d_{52}$
	One discoidal boulder ~350 mm	d_{67}
	One elongate cobble ~250 mm	d_{52}
P4	Mostly cobbles ≤250 mm	$\leq d_{52}$
R10	Cobble deposits, mostly <150 mm	$<d_{36}$
P11	Cobbles ≤200 mm	$\leq d_{54}$
	One boulder 490×450×240 mm	d_{69}
	Two platy boulders ~350 mm	d_{68}
R12	Mostly cobbles ~200 mm	d_{58}
	One boulder ~400 mm	d_{77}

P and R denote numbered pools and riffles, respectively.

A series of analytical methods was used to estimate the annual exceedance probabilities (AEP) of the extreme rainstorm and resultant flood. The results are presented here in summary form, with details given by Jansen (2001). The rainfall across Sandy Creek catchment on the 18th December 1992 ranged between the two depths recorded in the upper and lower parts of the catchment: 102 and 133 mm, respectively. The storm was concentrated over 3 to 4 h (Mr. P. Adams, local station manager, personal communication, Dec. 1992). Based on frequency analyses of 24-h rainfall data from 3 long-term records within a 35 km radius (viz. Fowlers Gap, Sturts Meadows and Corona), coupled with rainfall depth–intensity–frequency analyses (Pilgrim, 1987; Pilgrim et al., 1987), the rainstorm represents a maximum AEP of 2×10^{-2}, but is probably less than 5×10^{-3}.

Flood debris swept along by floodwaters produced clear evidence of peak stage, and peak flood discharge was estimated at 170 m^3/s using methods detailed in the next section. Four different methods were employed to estimate the recurrence frequency of this flood: partial flood series analysis of the adjoining gauged catchment (Homestead Creek), a unit hydrograph method (Cordery, 1987), the rational method (Pilgrim, 1987), and a regional-regression method (MacQueen, 1978, 1979). Based on these analyses, the 1992 flood was determined to approximate the 100-year flood magnitude (AEP~10^{-2}).

5.2. Palaeohydrology

Jansen and Brierley (2004) propose a late Holocene palaeoflood history for Sandy Creek gorge based on stratigraphic analyses and radiocarbon dating of the pool-fill deposits in the lower gorge (Fig. 4a). The chronology of these floods indicates long stable intervals of 10^2–10^3 years punctuated by episodic flushing events. The sequence of erosional and depositional episodes is summarised in Table 3. Four flow magnitudes (or index floods) are proposed to represent the full spectrum of formative floods over the late Holocene: Q_{bf} (bankfull flow), Q_{100} (the 1992 flood), Q_{p2} (a major palaeoflood equating with 'erosion episode 4' in Table 3), and Q_{p1} (a 'superflood' equating with 'erosion episode 1' in Table 3). The following hydraulic analyses aim (1) to determine the peak discharge of the index floods based on stage indicators, and (2) to determine downstream trends in mean shear stress so as to evaluate bed material mobility for each of the index floods.

5.3. Flow modelling: methods and results

Flow modelling was conducted using a step-backwater model, HEC-RAS (2001), which is based on conservation of mass and energy associated with steady, gradually varied flow. For a series of representative cross-sections down-valley, an energy-balanced water-surface profile is calculated as a function of discharge, roughness and flow geometry (Feldman, 1981). HEC-RAS was chosen over other more sophisticated two- and three-dimensional models because of its simple and well-tested set of assumptions that are relatively easy to evaluate for geomorphologic applications (Miller and Cluer, 1998).

The modelling run extends for 4.4 km including R4 to R14 (Fig. 1). Cross-sections, located to optimise definition of downstream changes in channel and valley geometry, were surveyed with a theodolite level and tied into a detailed long profile survey. HEC-RAS requires an estimate of energy loss in terms of Manning's (1895) roughness coefficient (n), which incorporates the effects of bed roughness, vegetation drag and irregularities in bed and channel morphology that further dissipate flow energy via turbulence (Jarrett, 1984; Tinkler, 1997; Miller and Cluer, 1998). In steep channels, roughness tends to be proportional to gradient and inversely proportional to flow depth or relative submergence (i.e. the ratio of flow depth to clast size). Derived from Rocky Mountain streams with relative submergence ratios comparable to those in Sandy Creek, the Jarrett (1984) equation was chosen to predict reach-scale roughness: $n = 0.32\ S^{0.38}\ R^{-0.16}$, where S is channel gradient and R is hydraulic radius. Inputs of Manning's n were varied ($n \sim 0.08$–0.04) according to reach-scale changes in gradient and depth.

The model was run in 'mixed regime' mode, and expansion and contraction loss coefficients were set to 0.3 and 0.1, respectively. Because flow competence evaluations based on section-averaged hydraulics tend to overestimate palaeodischarge (Carling, 1986), the cross-sections were partitioned to delimit local hydraulic conditions over the riffle coarse locales. Detailed stage data measured at each of 26 cross-sections following the 1992 flood (Q_{100}) were used to evaluate water-surface profile outputs from HEC-RAS, with discharge adjusted iteratively to match the field evidence. Stage-indicators were contained within a ±10% envelope of modelled discharge at most cross-sections (Fig. 6). For the other index floods, initial cross-sections were set to critical flow depth and various discharge inputs were tested until a best-fit was achieved with the field evidence. Water-surface profiles predicted for the four index floods are presented in Fig. 6, and key outputs are summarised in Table 4. Consistent with observations of steepland streams elsewhere (e.g. Tinkler, 1997; Grant, 1997), widespread transcritical flow was predicted, including possible hydraulic jumps at constrictions near R10 and R13, and upstream of R4 (Figs. 4a and 6).

Fig. 7 presents the predicted mean shear stress and unit discharge compared with threshold conditions on the riffles according to Komar (1987) and Ferguson (1994). The following is an overview of the hydraulic conditions and bed material mobility for each of the index floods.

5.3.1. Q_{bf} (20 m^3/s)

Although the bankfull discharge concept as applied to alluvial channels is not strictly applicable to bedrock gorges, 'bankfull' geometry of some sort is defined by

Table 3
Major erosional and depositional episodes in Sandy Creek gorge over the late Holocene

Erosional/depositional episode	Flood magnitude	Estimated age (cal BP)
Erosion episode 1	Extreme	3360–1860
Erosion episode 2	High	1530–960
Erosion episode 3	Moderate	740–570
Erosion episode 4	Moderate	~300
Deposition	Low	570–260
Post-settlement regime	Low-moderate	Post-AD 1860s

Estimated ages derive from a ^{14}C chronology given by Jansen and Brierley (2004).

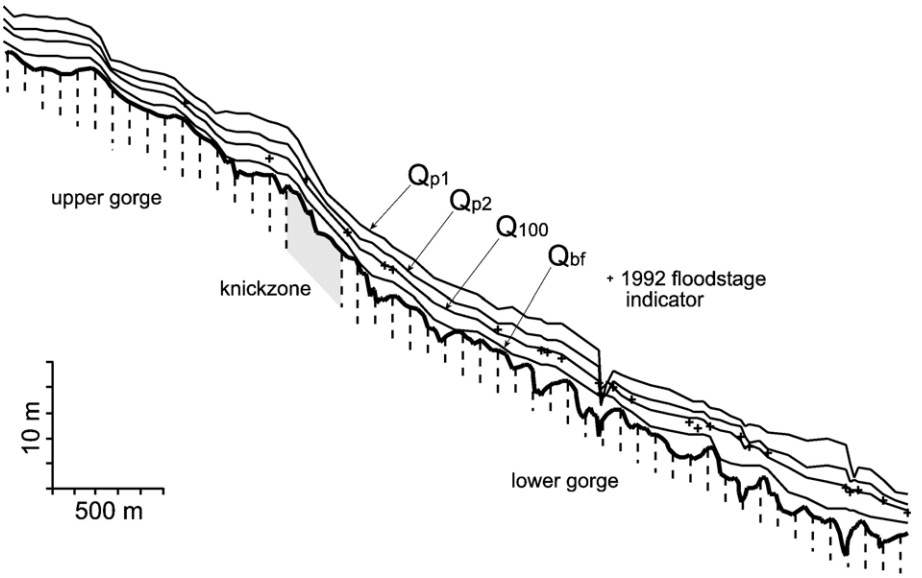

Fig. 6. Water surface profiles (flow from left to right) predicted by HEC-RAS for the four index floods: Q_{bf}, Q_{100}, Q_{p2}, and Q_{p1}. The modelled discharge for Q_{100} is contained within ±10% of the field-observed stage indicators at most cross-sections. Note the potential hydraulic jumps generated at bedrock constrictions near R10 and R13, and upstream of R4.

1–2 m high alluvial benches at pools, which confine a relatively frequent discharge to a cross-section that is adjusted to those flows (Jansen and Brierley, 2004). This 'bankfull' discharge is competent to entrain up to medium-sized cobbles, but falls well short of threshold conditions for boulder transport (Q_{bf} is therefore not included in Fig. 7).

5.3.2. Q_{100} (170 m^3/s)

The 1992 flood was probably among the largest floods since European settlement in the 1860s and is equated with the 100-year flood (i.e. AEP = 10^{-2}). Resulting from 3.8 $m^3/s/km^2$ of runoff generation across the catchment, this flood inundated the narrow coarse-grained floodplains but caused little lasting change. Hydraulic and sediment transport modelling predicts entrainment of small boulders: d_{50} clasts were probably mobile at 7 of the 11 riffles (Fig. 7), and coarse modes were probably mobile on 1 or 2 riffles at most. These results are consistent with post-1992-flood field observations of transported gravels in the d_{50}–d_{60} range (Table 2). Thus, while median clast sizes are likely to be mobilised in a 100-year flood, the structural frameworks of the riffles remain largely unaffected.

5.3.3. Q_{p2} (350 m^3/s)

The Q_{p2} flood magnitude represents a major palaeoflood equating with 'erosion episode 4' in

Table 4
Summary results of the HEC-RAS flow modelling (R4–R14) for all cross-sections

		Q_{bf}	Q_{100}	Q_{p2}	Q_{p1}
Q, peak discharge (m^3/s) upstream and downstream of R9 [a]		15, 20	120, 170	280, 350	600, 750
n, Manning's roughness coefficient [b]	Range	0.056–0.082	0.051–0.070	0.048–0.066	0.046–0.065
R, hydraulic radius (m)	Mean ± 1σ	1.0 ± 0.5	2.2 ± 0.7	2.8 ± 0.7	4.0 ± 1.0
F, channel Froude number	Mean ± 1σ	0.43 ± 0.26	0.61 ± 0.32	0.66 ± 0.21	0.78 ± 0.36
	% critical [c]	~10	~20	~25	~40
V, channel mean flow velocity (m/s)	Mean ± 1σ	1.08 ± 0.42	2.65 ± 1.09	3.40 ± 0.93	4.65 ± 1.69
Mobile clast size fraction [d]	%	d_5–d_{16}	d_{50}	d_{50}–d_{84}	d_{95}–d_{5x}
	mm	~100	~350	~600	~1500

[a] Two separate discharges were modelled upstream and downstream of the tributary input at R9.
[b] Calculated from Jarrett (1984): $n = 0.32\ S^{0.38} R^{-0.16}$; the upper roughness value corresponds to the knickzone reach.
[c] Approximate proportion of the channel length predicted with transcritical flow conditions.
[d] The clast size percentile predicted to be mobile on at least half the riffles.

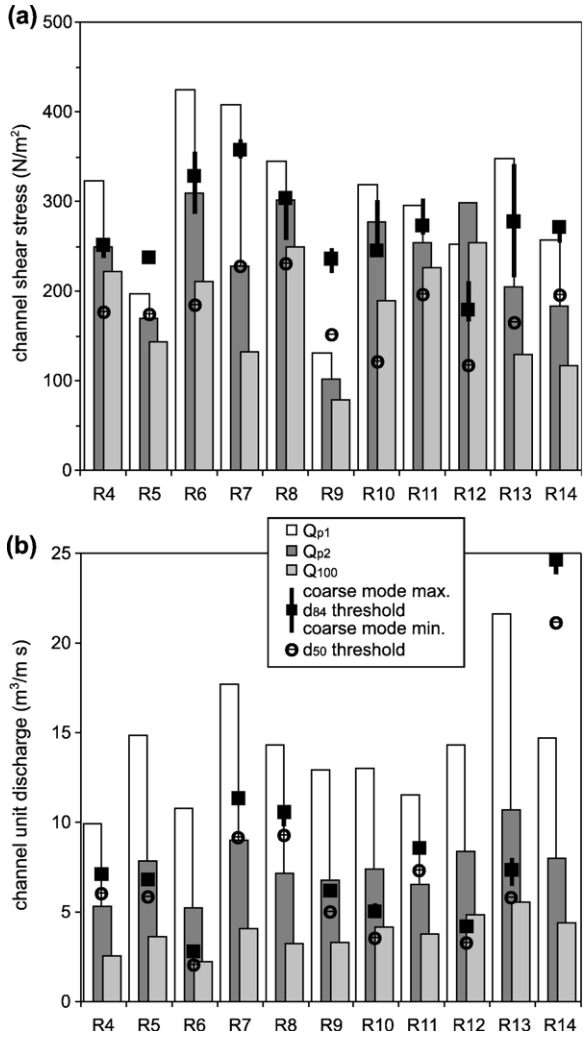

Fig. 7. Thresholds of clast mobility over riffles (R4–R14) relative to predicted flow competence for Q_{p1} (750 m^3/s), Q_{p2} (350 m^3/s), and Q_{100} (170 m^3/s) flow magnitudes in terms of (a) critical mean shear stress, τ_c (Komar, 1987); and (b) critical unit discharge, q_c (Ferguson, 1994). Reach-averaged $\tau_{c(d_{84})}$ is essentially constant across riffles of the upper gorge (R4–R5) and lower gorge (R6–R14): 244 ($1\sigma = 9$) N/m^2; and 274 ($1\sigma = 52$) N/m^2, respectively. For all riffles, mean $\tau_{c(d_{84})}$ equals 268 ($1\sigma = 48$) N/m^2. Note that Q_{bf} has insufficient competence to entrain riffle boulders.

Table 3, which eroded the pool-fill sequences at about 300 cal. BP (Jansen and Brierley, 2004). The impacts of saltating gravel or large woody debris during this flood caused flood scars on senescent *Eucalyptus camaldulensis* trees indicating a flowstage at least 1.1 m above the Q_{100} flood peak in 1992. The modelling predicts that d_{50} clasts are likely to be mobile at 10 riffles, and coarse modes mobile at 8 of the 11 riffles, which is close to a fully mobile bed (Fig. 7).

5.3.4. Q_{p1} (750 m^3/s)

Two lines of evidence indicate the passage of extreme floods in Sandy Creek gorge: deposits of large imbricated boulders (Fig. 3b), and slackwater sediments found draping the lower gorge strath terrace. Extreme floods are responsible for episodic removal of the pool-fills and scour to bedrock (cf. Schick, 1974; Jansen and Brierley, 2004); therefore, the most recent such flood predates the pool-fill basal deposits (i.e. 'erosional episode 1' in Table 3). Step-backwater modelling of stages corresponding to the terrace drapes is used to estimate the Q_{p1} discharge. The resultant 750 m^3/s flood is predicted to entrain riffle boulders 1 to 2 m in diameter and all except one of the riffle crests are likely to be mobile (Fig. 7). The lack of bed material mobility at R14 reflects its position beyond the rangefront on the depositional piedmont.

6. Discussion

6.1. Formative floods and mobility of coarse alluvial cover

Unlike alluvial channels, in which the formative or 'channel-forming' discharge is typically approximated by bankfull flow (e.g. Pickup and Warner, 1976; Emmett and Wolman, 2001), no easily measured quantity relating to geomorphic-effectiveness has been clearly identified for mixed bedrock–alluvial channels. Highly resistant flow boundaries comprising bedrock and/or coarse alluvium give rise to high erosion thresholds, and so formative flows will be of high magnitude and low frequency. Furthermore, channel dimensions and coarse sedimentary deposits shaped during rare large floods persist over long intervals and tend to constrain stream processes associated with smaller, frequent flows (Baker, 1977).

It is proposed here that the size percentile with the fastest rate of systematic downstream-fining indicates the coarsest fraction of *transient* alluvium in rivers supplied with coarse sediment (e.g. Fig. 5d). Accordingly, in Sandy Creek gorge the d_{68}–d_{88} size fraction represents the coarsest transient bed materials, matching approximately the riffle coarse modes (i.e. d_{75}–d_{95}, Fig. 5c). In the absence of detailed sediment transport and flow data that allow calculation of the discharge increment associated with transporting the most bed load yield (i.e. the *effective* discharge), formative discharge might be reasonably indicated by threshold conditions for the d_{84} ($\tau_{c(d_{84})}$) or other size fraction with the fastest rate of downstream fining. Coarser blocks (e.g. d_{5x}) plucked from nearby joints reflect the joint-

spacing attributes of their local bedrock sources rather than local flow competence. Such blocks are probably broken down in situ by impacts of passing bed load before being transported as smaller fragments. Using $\tau_{c(d_{84})}$ to indicate the formative flow is consistent with sediment transport studies of coarse-bed streams that use d_{84} or d_{90} to represent bed structure, inferring that such clasts are the principal roughness components and so are most influential on channel gradient and morphology (e.g. Howard, 1980; Jackson and Beschta, 1982; Prestegaard, 1983; Hey and Thorne, 1986; Howard, 1987; Grant et al., 1990).

Few studies report τ_b and τ_c values in the context of formative discharge for a mixed bedrock–alluvial river. Extreme τ_b values of 10^3–10^4 N/m^2 are estimated for cataclysmic floods (e.g. Baker and Kale, 1998), though such events far exceed what is normally regarded as channel forming. Much lower values are reported elsewhere. For instance, Snyder et al. (2003) estimate τ_b at ~100–200 N/m^2 for a rare large flood in Fall Creek, New York, and argue that this just exceeded τ_c for bedrock plucking.

Fig. 8 presents flow modelling results for the formative discharge (Q_{p2}=350 m^3/s) predicting a total τ_b peak exceeding 500 N/m^2 along the knickzone, and peaks of ~200–300 N/m^2 in the upper and lower gorge. Using the critical-stress approach (Fig. 7a), $\tau_{c(d_{84})}$ must exceed 180–360 N/m^2 for crest mobility on the 11 riffles surveyed. The associated threshold discharge ($Q_c=q_cW$) calculated using the critical-discharge approach spans 115–580 m^3/s (Fig. 7b), suggesting that extensive reworking of riffles is restricted to floods roughly twice the magnitude of Q_{100} and that formative floods may be spaced by intervals of several centuries (AEP ~10^{-2}–10^{-3}). The predictions of τ_c show that bankfull discharge is an order of magnitude short of discharges necessary to entrain even median clast sizes in Sandy Creek gorge; thus, Q_{bf} is clearly an inadequate proxy for the formative flood here. The same may hold for mixed bedrock–alluvial streams more widely. Several studies of boulder-bed cascade, step-pool, and riffle-pool channels report that bed-forming clasts are mobilised only by rare high-magnitude floods with recurrence intervals of 50–100 years or more (e.g. O'Connor et al., 1986; Baker and Pickup, 1987; Whittaker, 1987; Grant et al., 1990; Chin, 1998). Any new formulation of bedrock incision laws must account for the high magnitude and low frequency of formative events found in many mixed bedrock–alluvial channels.

6.2. Mutual adjustments between lithology, channel morphology and alluvial cover

For mixed bedrock–alluvial streams in which bedrock plucking is the chief erosion process, two kinds of critical erosion threshold (τ_c) exist: (1) the entrainment threshold for coarse boulders in bedforms lining the channel (i.e. the transport-limited condition, $\tau_{c(TL)}$), and (2) the threshold for plucking coarse blocks from bedrock joints (i.e. the detachment-limited condition, $\tau_{c(DL)}$). The long history of attempts to quantify factors affecting initial motion of particles–including clast lithology, shape and size distribution, packing and orientation within bedform structures, and shielding effects–has yielded some success (Gomez and Church, 1989; Buffington and Montgomery, 1997). Whereas the

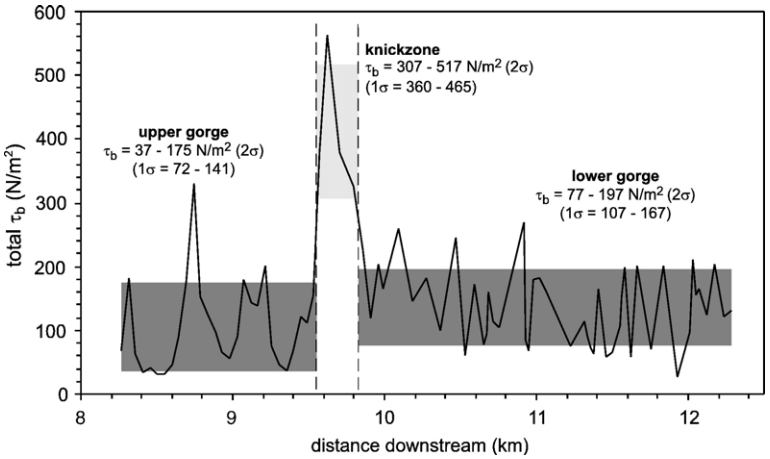

Fig. 8. Downstream variation in total mean shear stress (τ_b) as predicted by HEC-RAS modelling for the formative discharge (350 m^3/s). Reach-averaged trends (shading spans 2σ errors) indicate that τ_b is statistically constant across the upper and lower gorge, but significantly higher across the knickzone where the gorge meets resistant quartzites.

bedrock plucking problem has received attention only relatively recently and processes influencing $\tau_{c(DL)}$– such as physical and chemical weathering, sand-wedging, macroabrasion-driven rock fracture, local drag and lift forces, joint-spacing and dip-angle relative to flow trajectory–have proved difficult thus far to integrate into a quantitative mechanistic model (e.g. Annandale, 1995; Whipple et al., 2000).

There is no reason to expect that the ratio $\tau_{c(TL)}/\tau_{c(DL)}$ should equal unity; such a case implies a fully deformable flow boundary, as with alluvial channels, which we know does not apply to rivers incising hard rocks. Moreover, it may be that the $\tau_{c(TL)}/\tau_{c(DL)}$ relationship is an important determinant of transport-limited versus detachment-limited erosion at the reach-scale. In the case of the Sandy Creek knickzone, for instance, bedrock is exposed where $\tau_b > \tau_{c(TL)} < \tau_{c(DL)}$; whereas, in the transport-limited upper and lower gorge in which very stable bedforms mantle weak rocks, $\tau_b < \tau_{c(TL)} > \tau_{c(DL)}$ (and bedrock erosion is restricted to when $\tau_b > \tau_{c(TL)}$).

Generalising at the reach-scale, bedrock fluvial incision occurs via (1) knickzone propagation in which a steepened reach (or kinematic incisional wave) propagates upstream incising bedrock while transmitting base level fall through the drainage network—a non-steady state, transient response; and (2) uniform, or diffusive bed incision in which bedrock channel width, depth, and gradient mutually adjust to accommodate river incision in response to substrate resisting forces. A band of resistant rocks, for instance, commonly causes channel constriction and steepening, thereby maintaining a uniform incision rate across adjoining reaches cut in weaker rocks. Such steepened reaches in the river profile are non-propagating knickzones and may form part of steady-state topography (Hack, 1957, 1975).

The latter style of fluvial incision appears to apply in Sandy Creek gorge. Equivalence of mean channel width, gradient, and proportion of alluvial cover upstream and downstream of the knickzone suggests that channel morphology is tuned to maintaining a spatially uniform rate of incision across reaches of varying resistance. Such a steady state arrangement of uniform incision across the three reaches implies that mean shear stress (τ_b) during formative events varies downstream, according to the relationship:

$$\tau_{b(TL)}/\tau_{c(TL)} = \tau_{b(DL)}/\tau_{c(DL)} \quad (6)$$

where $\tau_{b(TL)}$ and $\tau_{b(DL)}$ are average boundary shear stress in transport-limited and detachment-limited reaches, respectively. Fig. 8 shows that for the formative discharge reach-averaged τ_b is essentially equivalent in the upper and lower gorge, separated by a prominent spike where the gorge narrows and steepens across resistant quartzites along the knickzone. Likewise, $\tau_{c(d_{84})}$ values averaged across the upper and lower gorge riffles are also statistically equivalent (see Fig. 7 caption), indicating that the ratio on the left side of Eq. (6) holds for both these transport-limited reaches. Although $\tau_{c(DL)}$ for bedrock plucking along the knickzone was not directly quantified, it can be deduced from Eq. (6) that the knickzone erodes in pace with the upper and lower gorge and, therefore, reach-averaged $\tau_{c(DL)}$ is roughly balanced by τ_b at approximately 300–500 N/m^2 (Fig. 8).

The linearity of the bed profile in the lower gorge is striking given that several quartzite units (1–5 m thick) cause abrupt local constrictions in channel width (Figs. 2 and 4). A constant incision rate is apparently maintained across these thin resistant outcrops by concentrating shear stress via channel width adjustment alone (these peaks are shown in terms of unit discharge in Fig. 4c). The greater thickness (55 m) of the quartzite unit outcropping along the knickzone presumably requires both narrowing *and* steepening to generate shear stress sufficient to maintain uniform incision relative to the upper and lower gorge. Moreover, these harder rocks cause the channel to occupy the full width of the gorge, suggesting insufficient excess shear stress for strath formation (Merritts et al., 1994; Pazzaglia et al., 1998). A stream's capacity to erode resistant bedrock by constricting flow width without steepening is governed by the magnitude of τ_b relative to τ_c. Setting aside transient response to base level fall, a smoothly concave-up river profile cut across diverse rocks is possible only in rivers with a large excess of shear stress (i.e. $\tau_b \gg \tau_c$)(Hovius, 2000). Accordingly, the general lack of concavity found in the profiles of dryland bedrock rivers chiefly reflects the downstream decline in excess τ_b (due to the typical falling rather than rising discharge downstream), which allows harder rocks to exert greater control on profile shape.

In addition to lithologic controls on channel morphology the presence of coarse alluvial cover is crucial to river profile shape (Hack, 1957; Howard et al., 1994; Howard, 1998; Sklar and Dietrich, 1998; Gasparini et al., 2004). Sklar and Dietrich (2001) argue that because small shifts in channel gradient trigger large shifts in bedrock exposure and therefore also in the rate of bedrock incision, rapidly incising rivers or those incising resistant rocks will have steeper gradients, but also much more extensive bedrock exposure. Recognising this additional means of channel

adjustment they suggest that relief may be less sensitive to differences in lithology or uplift rate than previously indicated by simple applications of the stream power law (e.g. Whipple and Tucker, 1999). This is apparent in Sandy Creek where uniform incision across diverse rocks is accommodated via adjustments to channel morphology and the alluvial cover: the knickzone features 2-fold channel steepening, halving of channel width and greater than 3-times more extensive bedrock exposure relative to the upper and lower gorge (Fig. 2). Further complexity emerges when the alluvial cover is viewed at the sub-reach scale. Rather than being uniformly distributed (cf. Sklar and Dietrich's saltation-abrasion model), the coarse bed materials tend to organise into macrobedforms that reflect downstream variations in flow competence and the underlying rock floor topography (Fig. 4). As in Sandy Creek, coarse boulder deposits capping convexities in the rock floor profile are also described from the Herbert gorge, in NE Queensland (Wohl, 1992b), and it may be that such an arrangement is common to many bedrock systems, especially those undergoing low rates of incision.

7. Implications for bedrock river incision in post-orogenic landscapes

Despite more than 90% of the Earth's land surface being essentially post-orogenic, research on the erosional dynamics of bedrock rivers and their role in the evolution of topography has focused mainly on tectonically active settings. The Barrier Range, in contrast, represents a Proterozoic orogen at an advanced stage of topographic decay with maximum relief of about 300 m, which after $\sim 10^8$ years of subaerial erosion is probably at least 5–10% of what once existed. While still triggering a slight orographic effect, this landscape represents the end-member of post-orogenic settings—an extremeness reinforced by aridity, which itself reflects low relief, continental interiors. This is very stable terrain that delivers low sediment yields to rivers with low sediment transport capacity. Bedrock fluvial incision is certainly active albeit episodic and exceedingly slow (<5 m/Ma).

Since Whipple and Tucker's (2002) suggestion that decreasing surface uplift during post-orogenic topographic decay might drive a shift to channel-bed alluviation and transport-limited conditions in river networks, it has been shown that inclusion of even relatively low critical erosion thresholds greatly affects the topographic predictions of surface process models (e.g. Snyder et al., 2003; Tucker, 2004). Baldwin et al. (2003) successfully simulate the lengthy timescales of post-orogenic topographic decay by incorporating an erosion threshold, stochastic flood distribution and isostatic rebound into their detachment-limited stream power incision model, thus offering a predominantly geomorphic explanation for the topographic persistence of ancient orogenic belts, such as the Appalachians and east Australian highlands. If, as suggested by Whipple and Tucker (2002) and Baldwin et al. (2003), the erosional efficiency (K in Eq. (1)) of a bedrock channel declines with ongoing topographic decay, then Sandy Creek gorge ought to exemplify a very 'inefficient' system (cf. Stock and Montgomery, 1999; van der Beek and Bishop, 2003). Accordingly, low erosional efficiency might manifest in some combination of (1) coarse bed texture (i.e. high erosion thresholds), (2) low frequency of formative floods, and (3) declining bedrock exposure (plus thickening of alluvial cover). Firstly, results here support the notion that erosion thresholds may be very substantial in rivers draining post-orogenic terrain. Observations of large blocks concentrated on the channel bed under low sediment flux conditions are consistent with experimental and field studies showing that bed texture tends to coarsen with declining rates of sediment supply (e.g. Howard, 1987; Dietrich et al., 1989; Buffington and Montgomery, 1999). Secondly, geomorphically effective flows in Sandy Creek gorge are spaced at very long intervals, with AEP values of 10^{-2}–10^{-3}, and such may be representative of post-orogenic settings, especially those of arid continental interiors. Simple stream power-based bedrock incision approaches that use K (Eq. (1)) to represent a geomorphically effective 0.2–0.1 AEP flood are unlikely to be a valid representation in these landscapes.

Concerning the third point, extensive bedrock exposure in Sandy Creek gorge (27–95% per reach) backed by observations of ubiquitous bedrock-dominated rivers in post-orogenic terrain elsewhere appears contrary to predictions of channel-bed alluviation during advanced stages of topographic decay (e.g. Pazzaglia et al., 1998; Whipple and Tucker, 2002; Baldwin et al., 2003). Bedrock channel exposure is a function of excess sediment transport capacity relative to sediment supply. Yet, excess transport capacity is easily achieved when channels receive and generate negligible volumes of sediment over long periods. Accordingly, the prevalence of bedrock exposure can be explained by the generally low rates of sediment supply to channels due to slow physical weathering. Howard et al. (1994) propose three causes of mixed bedrock–alluvial rivers: (1) high erosion rate and/or resistant rocks, (2) climatic fluctuations, and (3) knickzone propagation. The low sediment

flux produced in weathering-limited landscapes provides a fourth cause.

Maintenance of extremely slow bedrock incision despite abundant outcrop suggests aspects of 'erosional inefficiency' hitherto not widely considered in studies of bedrock river incision. Sklar and Dietrich (1998, 2001) convincingly show that a certain fraction of alluvial cover optimises the rate of bedrock fluvial incision; increased cover shields the rock floor from further erosion, whereas reduced sediment provides insufficient tools for abrasion and related erosional processes to operate. The influence of more complex aspects of channel morphology: macrobedforms and spatial patterns of alluvial cover are yet to be evaluated, but the present study suggests that such factors will be found to be important.

The role of coarse alluvial cover in Sandy Creek gorge can be regarded at two scales: (1) modulation of bedrock exposure at the reach-scale, coupled with adjustment to channel width and gradient, accommodates uniform incision across rocks of different erodibility in steady-state fashion; and (2) at the sub-reach scale where coarse boulder deposits (corresponding to τ_b minima) cap rock-floor convexities, thereby restricting bedrock incision to rare large floods. At both scales mutual adjustments between lithology, channel morphology and the discontinuous alluvial cover appear to distribute energy expenditure in a spatially uniform manner (Langbein and Leopold, 1964; Wohl and Merritt, 2001).

Because coarse alluvial cover is common to both rapidly incising and slowly incising mixed bedrock–alluvial rivers, an intriguing question is how a partial alluvial cover might be spatially distributed to either optimise or impede the rate of bedrock incision and what, if any, are the fundamental controls driving such behaviour. Observations here suggest that the small volume of very stable bed materials is distributed so as to maximise flow resistance and energy dissipation, and minimise the rate of bedrock fluvial incision over time.

Acknowledgements

This research stems from the author's doctoral work at the Department of Physical Geography, Macquarie University. Gary Brierley is thanked for his enduring support at that time. The paper was written at the University of Glasgow during an Anglo-Australian Postdoctoral Fellowship funded by the Royal Academy of Engineering. Thanks to Derek Fabel for arranging a Visiting Fellowship to complete this work at the Research School of Earth Sciences, Australian National University. Paul Bishop, Trevor Hoey, and Andrew J. Miller are thanked for their insightful critiques. The author acknowledges the Traditional Owners of this country.

References

Annandale, G.W., 1995. Erodibility. Journal of Hydraulic Research 33, 471–494.

Ashworth, P.J., Ferguson, R.I., 1989. Size-selective entrainment of bed load in gravel bed streams. Water Resources Research 25, 627–634.

Baker, V.R., 1977. Stream-channel response to floods, with examples from central Texas. Geological Society of America Bulletin 88, 1057–1071.

Baker, V.R., 1978. Large-scale erosional and depositional features of the Channeled Scabland. In: Baker, V.R., Nummedal, D. (Eds.), The Channeled Scabland. National Aeronautics and Space Administration, Washington, DC, pp. 81–115.

Baker, V.R., 1984. Flood sedimentation in bedrock fluvial systems. In: Koster, E.H., Steel, R.J. (Eds.), Sedimentology of Gravels and Conglomerates. Canadian Society of Petroleum Geologists, Calgary, pp. 87–98.

Baker, V.R., 1988. Flood erosion. In: Baker, V.R., Kochel, R.C., Patton, P.C. (Eds.), Flood Geomorphology. John Wiley and Sons, New York.

Baker, V.R., Kale, V.S., 1998. The role of extreme floods in shaping bedrock channels. In: Tinkler, K.J., Wohl, E.E. (Eds.), Rivers Over Rock: Fluvial Processes in Bedrock Channels. Geophysical Monograph, vol. 107. American Geophysical Union, Washington, DC, pp. 153–165.

Baker, V.R., Pickup, G., 1987. Flood geomorphology of the Katherine Gorge, Northern Territory, Australia. Geological Society of America Bulletin 98, 635–646.

Baldwin, J.A., Whipple, K.X., Tucker, G.E., 2003. Implications of the shear stress river incision model for the timescale of post-orogenic decay of topography. Journal of Geophysical Research 108, doi:10.1029/2001JB000550.

Bathurst, J.C., 1987. Critical conditions for bed material movement in steep, boulder-bed streams. In: Beschta, R.L. (Ed.), Erosion and Sedimentation in the Pacific Rim. International Association of Hydrological Sciences Publication, vol. 165, pp. 309–318.

Bathurst, J.C., Graf, W.H., Cao, H.H., 1983. Initiation of sediment transport in steep channels with coarse bed material. In: Multlu Summer, B., Muller, A. (Eds.), Mechanics of Sediment Transport. Proceedings of Euromech, vol. 156. A.A. Balkema, Rotterdam, pp. 207–213.

Bathurst, J.C., Graf, W.H., Cao, H.H., 1987. Bedload discharge equations for steep mountain rivers. In: Thorne, C.R., Bathurst, J.C., Hey, R.D. (Eds.), Sediment Transport in Gravel-Bed Rivers. John Wiley and Sons, pp. 453–457.

Beaumont, C., Fullsack, P., Hamilton, J., 1992. Erosional control of active compressional orogens. In: McClay, K.R. (Ed.), Thrust Tectonics. Chapman and Hall, New York, pp. 1–18.

Bierman, P.R., Turner, J., 1995. ^{10}Be and ^{26}Al evidence for exceptionally low rates of Australian bedrock erosion and the likely existence of pre-Pleistocene landscapes. Quaternary Research 44, 378–382.

Brayshaw, A.C., 1984. Characteristics and origin of cluster bedforms in coarse-grained alluvial channels. In: Koster, E.H., Steel, R.J. (Eds.), Sedimentology of Gravels and Conglomerates. Canadian Society of Petroleum Geologists, pp. 77–85.

Brierley, G.J., Hickin, E.J., 1985. The downstream gradation of particle sizes in the Squamish River, British Columbia. Earth Surface Processes and Landforms 10, 597–606.

Buffington, J.M., Montgomery, D.R., 1997. A systematic analysis of eight decades of incipient motion studies, with special reference to gravel-bed rivers. Water Resources Research 33, 1993–2029.

Buffington, J.M., Montgomery, D.R., 1999. Effects of sediment supply on surface textures of gravel-bed rivers. Water Resources Research 35, 3523–3530.

Bureau of Meteorology, 1988. Climatic Atlas of Australia. Australian Government Publishing Service, Canberra.

Carling, P., 1986. The Noon Hill flash floods, July 17th 1983: hydrological and geomorphological aspects of a major formative event in an upland landscape. Transactions of the Institute of British Geographers 11, 105–118.

Chin, A., 1998. On the stability of step-pool mountain streams. Journal of Geology 106, 59–69.

Church, M., Kellerhals, R., 1978. On the statistics of grain size variation along a gravel river. Canadian Journal of Earth Sciences 15, 1151–1160.

Cordery, I., 1987. The unit hydrograph method of flood estimation. In: Pilgrim, D.H. (Ed.), Australian Rainfall and Runoff: A Guide to Flood Estimation, vol. 1. Institution of Engineers, Barton, ACT, Australia, pp. 151–172.

Costa, J.E., 1983. Paleohydraulic reconstruction of flash flood peaks from boulder deposits in the Colorado Front Range. Geological Society of America Bulletin 94, 986–1004.

Dietrich, W.E., Kirchner, J.W., Ikeda, H., Iseya, F., 1989. Sediment supply and the development of the coarse surface layer in gravel-bedded rivers. Nature 340, 215–217.

Emmett, W.W., Wolman, M.G., 2001. Effective discharge and gravel-bed rivers. Earth Surface Processes and Landforms 26, 1367–1368.

Feldman, A.D., 1981. HEC models for water resources system simulation theory and experience. Advances in Hydroscience 12, 297–923.

Ferguson, R.I., 1994. Critical discharge for entrainment of poorly sorted gravel. Earth Surface Processes and Landforms 19, 179–186.

Gale, S.J., 1992. Long-term landscape evolution in Australia. Earth Surface Processes and Landforms 17, 323–343.

Gasparini, N.M., Tucker, G.E., Bras, R.L., 2004. Network-scale dynamics of grain-size sorting: implications for downstream fining, stream-profile concavity, and drainage basin morphology. Earth Surface Processes and Landforms 29, 401–421 (10.1002/esp.1031).

Gibson, D.L., 2000. Post-early Cretaceous landform evolution along the western margin of the Bancannia Trough, western NSW. Australian Rangeland Journal 22, 32–43.

Gilbert, G.K., 1877. Report on the Geology of the Henry Mountains. United States Geographical and Geological Survey of the Rocky Mountains Region. United States Government Printing Office, Washington, DC.

Gomez, B., Church, M., 1989. An assessment of bed load sediment transport formulae for gravel bed rivers. Water Resources Research 25, 1161–1186.

Grant, G.E., 1997. Critical flow constrains flow hydraulics in mobile-bed streams: a new hypothesis. Water Resources Research 33, 349–358.

Grant, G.E., Swanson, F.J., Wolman, M.G., 1990. Pattern and origin of stepped-bed morphology in high gradient streams, Western Cascades, Oregon. Geological Society of America Bulletin 102, 340–352.

Hack, J.T., 1957. Studies of longitudinal stream profiles in Virginia and Maryland. United States Geological Survey Professional Paper 294-B.

Hack, J.T., 1975. Dynamic equilibrium and landscape evolution. In: Melhorn, W.N., Flemal, R.C. (Eds.), Theories of Landform Development. State University of New York Press, Binghamton, pp. 87–102.

Hancock, G.S., Anderson, R.S., Whipple, K.X., 1998. Beyond power: bedrock river incision process and form. In: Tinkler, K.J., Wohl, E.E. (Eds.), Rivers Over Rock: Fluvial Processes in Bedrock Channels. Geophysical Monograph, vol. 107. American Geophysical Union, Washington, DC, pp. 35–60.

HEC-RAS, 2001. Hydrologic Engineering Center-River Analysis System, v. 3.0.1 User's Manual. U.S. Army Corps of Engineers, Davis, California.

Hey, R.D., Thorne, C.R., 1986. Stable channels with mobile gravel beds. Journal of Hydraulic Engineering 112, 671–689.

Hill, S.M., Eggleton, R.A., Taylor, G., 2003. Neotectonic disruption of silicified palaeovalley systems in an intraplate, cratonic landscape: regolith and landscape evolution of the Mulculca range-front, Broken Hill Domain, New South Wales. Australian Journal of Earth Sciences 50, 691–707.

Hovius, N., 2000. Macroscale process systems of mountain belt erosion. In: Summerfield, M.A. (Ed.), Geomorphology and Global Tectonics. John Wiley and Sons, Chichester, pp. 77–105.

Howard, A.D., 1980. Thresholds in river regimes. In: Coates, D.R., Vitek, J.D. (Eds.), Thresholds in Geomorphology. Allen and Unwin, Boston, pp. 227–258.

Howard, A.D., 1987. Modelling fluvial systems: rock-, gravel-, and sand-bed channels. In: Richards, K.S. (Ed.), River Channels: Environment and Process. Blackwell, Oxford, pp. 69–94.

Howard, A.D., 1998. Long profile development of bedrock channels: interaction of weathering, mass wasting, bed erosion, and sediment transport. In: Tinkler, K.J., Wohl, E.E. (Eds.), Rivers Over Rock: Fluvial Processes in Bedrock Channels. Geophysical Monograph, vol. 107. American Geophysical Union, Washington, DC, pp. 297–319.

Howard, A.D., Kerby, G., 1983. Channel changes in badlands. Geological Society of America Bulletin 94, 739–752.

Howard, A.D., Dietrich, W.E., Seidl, M.A., 1994. Modeling fluvial erosion on regional to continental scales. Journal of Geophysical Research 99 (B7), 13,971–13,986.

Inderbitzen, A.L., 1959. Gravels of Alameda Creek, California. Journal of Sedimentary Petrology 29, 212–220.

Jackson, W.L., Beschta, R.L., 1982. A model of two-phase bedload transport in an Oregon Coast Range stream. Earth Surface Processes and Landforms 7, 517–527.

Jansen, J.D., 2001. Bedrock Channel Morphodynamics and Landscape Evolution in an Arid Zone Gorge. Unpublished PhD thesis, Macquarie University, Sydney, Australia. 513 pp.

Jansen, J.D., Brierley, G.J., 2004. Pool-fills: a window to palaeoflood history and response in bedrock-confined rivers. Sedimentology 51, doi:10.1111/j.1365-3091.2004.00643.x.

Jarrett, R.D., 1984. Hydraulics of high-gradient streams. Journal of Hydraulic Engineering 110, 1519–1539.

Kieffer, S.W., 1985. The 1983 hydraulic jump in Crystal Rapid: implications for river-running and geomorphic evolution in the Grand Canyon. Journal of Geology 93, 385–406.

Knighton, A.D., 1980. Longitudinal changes in size and sorting of stream-bed material in four English rivers. Geological Society of America Bulletin 91, 55–62.

Knighton, A.D., 1998. Fluvial Forms and Processes: A New Perspective. Arnold, London. 383 pp.

Komar, P.D., 1987. Selective gravel entrainment and the empirical evaluation of flow competence. Sedimentology 34, 1165–1176.

Komar, P.D., 1996. Entrainment of sediments from deposits of mixed grain sizes and densities. In: Carling, P.A., Dawson, M.R. (Eds.), Advances in Fluvial Dynamics and Stratigraphy. John Wiley and Sons, Chichester, pp. 127–181.

Langbein, W.B., Leopold, L.B., 1964. Quasi-equilibrium states in channel morphology. American Journal of Science 262, 782–794.

Mabbutt, J.A., 1973. Geomorphology of fowlers gap station. In: Mabbutt, J.A. (Ed.), Lands of Fowlers Gap Station, New South Wales. Fowlers Gap Arid Zone Research Station Research Series, vol. 5, pp. 85–122.

MacQueen, A.D., 1978. Flood frequency in central Australia—a regional model, Water Division, Department of Transport and Works, Northern Territory.

MacQueen, A.D., 1979. A flood frequency model: Alice Springs area. Hydrology and Water Resources Symposium. Institution of Engineers, Perth, Australia, pp. 39–40.

Manning, R., 1895. On the flow of water in open channels and pipes. Transactions-Institution of Civil Engineers of Ireland 20, 161–207.

Martin, K.R., 1981. Deposition of the Precipice Sandstone and evolution of the Surat Basin in the Early Jurassic. Australian Petroleum Exploration Association Journal 21, 16–23.

Merritts, D.J., Vincent, K.R., Wohl, E.E., 1994. Long river profiles, tectonism, and eustasy: a guide to interpreting fluvial terraces. Journal of Geophysical Research 99 (B7), 14031–14050.

Miller, J.P., 1958. High mountain streams: effects of geology on channel characteristics and bed material. State Bureau of Mines and Mineral Resources/New Mexico Institute of Mining and Technology, Memoir, vol. 4. 57 pp.

Miller, J.R., 1991. The influence of bedrock geology on knickpoint development and channel-bed degradation along downcutting streams in south-central Indiana. Journal of Geology 99, 591–605.

Miller, A.J., Cluer, B.L., 1998. Modelling considerations for simulation of flow in bedrock channels. In: Tinkler, K.J., Wohl, E.E. (Eds.), Rivers Over Rock: Fluvial Processes in Bedrock Channels. Geophysical Monograph, vol. 107. American Geophysical Union, Washington, DC, pp. 61–104.

Molnar, P., England, P., 1990. Late Cenozoic uplift of mountain ranges and global climate change: chicken or egg? Nature 346, 29–34.

Neef, G., Bottrill, R.S., Ritchie, A., 1995. Phanerozoic stratigraphy of the northern Barrier Ranges, western New South Wales. Australian Journal of Earth Sciences 42, 557–570.

O'Connor, J.E., Webb, R.H., Baker, V.R., 1986. Paleohydrology of riffle-pool pattern development: Boulder Creek, Utah. Geological Society of America Bulletin 97, 410–420.

Parker, G., 1990. Surface-based bedload transport relation for gravel rivers. Journal of Hydraulic Research 28, 417–436.

Parker, G., Klingeman, P.C., McLean, D.G., 1982. Bedload and size-distribution in paved gravel-bed streams. Journal of the Hydraulics Division, American Society of Civil Engineers 108, 544–571.

Pazzaglia, F.J., Gardner, T.W., Merritts, D.J., 1998. Bedrock fluvial incision and longitudinal profile development over geologic time scales determined by fluvial terraces. In: Tinkler, K.J., Wohl, E.E. (Eds.), Rivers Over Rock: Fluvial Processes in Bedrock Channels. Geophysical Monograph, vol. 107. American Geophysical Union, Washington, DC, pp. 207–236.

Pickup, G., Warner, R.F., 1976. Effects of hydrologic regime on magnitude and frequency of dominant discharge. Journal of Hydrology 29, 51–75.

Pilgrim, D.H. (Ed.), 1987. Australian Rainfall and Runoff: A Guide to Flood Estimation (2 Vols.). Institution of Engineers, Barton, ACT, Australia. 374 pp.

Pilgrim, D.H., Kennedy, M.R., Rowbottom, I.A., Cordery, I., Canterford, R.P., Turner, L.H., 1987. Temporal patterns of rainfall bursts. In: Pilgrim, D.H. (Ed.), Australian Rainfall and Runoff: A Guide to Flood Estimation, vol. 1. The Institution of Engineers, Barton, ACT, Australia, pp. 43–52.

Prestegaard, K.L., 1983. Bar resistance in gravel bed streams at bankfull stage. Water Resources Research 19, 472–476.

Rana, S.A., Simons, D.B., Mahmood, K., 1973. Analysis of sediment sorting in alluvial channels. Journal of Hydraulics Division, American Society of Civil Engineers 99 (HY11), 1967–1980.

Raymo, M.E., Ruddiman, W.F., 1992. Tectonic forcing of late Cenozoic climate. Nature 359, 117–122.

Rhoads, B.L., 1989. Longitudinal variations in the size and sorting of bed material along six arid-region mountain streams. In: Yair, A., Berkowicz, S.M. (Eds.), Arid and Semi-Arid Environments—Geomorphological and Pedological Aspects. Catena Supplement, vol. 14, pp. 87–105.

Rice, S.P., 1998. Which tributaries disrupt downstream fining along gravel-bed rivers? Geomorphology 22, 39–56.

Schick, A.P., 1974. Formation and obliteration of desert stream terraces—a conceptual analysis. Zeitschrift für Geomorphologie. Supplementband 21, 88–105.

Schoklitsch, A., 1962. Handbuch des Wasserbaues. Springer-Verlag, Vienna.

Schumm, S.A., Stevens, M.A., 1973. Abrasion in place: a mechanism for rounding and size reduction of coarse sediments in rivers. Geology 1, 37–40.

Seidl, M.A., Dietrich, W.E., 1992. The problem of channel erosion in bedrock. In: Schmidt, K.H., de Ploey, J. (Eds.), Functional Geomorphology: Landform Analysis and Models. Catena Supplement, vol. 23, pp. 101–124.

Shields, A., 1936. Anwendung der Ahnlichkeitsmechanik und der Turbulenzforschung auf die Geschiebebewegung. Mitteilung der preussischen Versuchsanstalt fur Wasserbau und Schiffbau, 26, Berlin.

Sklar, L., Dietrich, W.E., 1998. River longitudinal profiles and bedrock incision models: stream power and the influence of sediment supply. In: Tinkler, K.J., Wohl, E.E. (Eds.), Rivers Over Rock: Fluvial Processes in Bedrock Channels. Geophysical Monograph, vol. 107. American Geophysical Union, Washington, DC, pp. 237–260.

Sklar, L.S., Dietrich, W.E., 2001. Sediment and rock strength controls on river incision into bedrock. Geology 29, 1087–1090.

Small, E.E., Anderson, R.S., 1995. Geomorphically driven Late Cenozoic rock uplift in the Sierra Nevada, California. Science 270, 277–280.

Snyder, N.P., Whipple, K.X., Tucker, G.E., Merritts, D.J., 2003. Importance of a stochastic distribution of floods and erosion thresholds in the bedrock incision problem. Journal of Geophysical Research 108 (B2), 2117, doi:10.1029/2001JB001655.

Sternberg, H., 1875. Untersuchungen über Langen- und Querprofil geschiebeführender Flüsse. Zeitschrift für Bauwesen 25, 483–506.

Stock, J.D., Montgomery, D.R., 1999. Geologic constraints on bedrock river incision using the stream power law. Journal of Geophysical Research 104, 4983–4993.

Thompson, S.M., Campbell, P.L., 1979. Hydraulics of a large channel paved with boulders. Journal of Hydraulic Research 17, 341–354.

Tinkler, K.J., 1971. Active valley meanders in south-central Texas, their wider implications. Geological Society of America Bulletin 82, 1783–1800.

Tinkler, K.J., 1997. Critical flow in rockbed streams with estimated values for Manning's n. Geomorphology 20, 147–164.

Troutman, B.M., 1980. A stochastic model for particle sorting and related phenomena. Water Resources Research 16, 65–76.
Tucker, G.E., 2004. Drainage basin sensitivity to tectonic and climatic forcing: implications of a stochastic model for the role of entrainment and erosion thresholds. Earth Surface Processes and Landforms 29, 185–205, doi:10.1002/esp1020.
Tucker, G.E., Bras, R.L., 2000. A stochastic approach to modeling the role of rainfall variability in drainage basin evolution. Water Resources Research 36, 1953–1964.
van de Graaf, W.J.E., 1981. Paleographic evolution of a rifted cratonic margin: SW Australia—discussion. Palaeogeography, Palaeoclimatology, Palaeoecology 34, 163–172.
van der Beek, P., Bishop, P., 2003. Cenozoic river profile development in the Upper Lachlan catchment (SE Australia) as a test of quantitative fluvial incision models. Journal of Geophysical Research 108 (B6), 2309, doi:10.1029/2002JB002125.
Veevers, J.J., 1984. Phanerozoic Earth History of Australia. Clarendon Press, Oxford.
Ward, C.R., Wright-Smith, C.N., Taylor, N.F., 1969. Stratigraphy and structure of the northeast part of the Barrier Ranges, New South Wales. Journal and Proceedings of the Royal Society of New South Wales 102, 57–71.
Wende, R., 1999. Boulder bedforms in jointed-bedrock channels. In: Miller, A.J., Gupta, A. (Eds.), Varieties of Fluvial Form. Wiley, Chichester, pp. 189–216.
Whipple, K.X., Tucker, G.E., 1999. Dynamics of the stream-power river incision model: implications for the height limits of mountain ranges, landscape response timescales, and research needs. Journal of Geophysical Research 104 (B8), 17661–17674.
Whipple, K.X., Tucker, G.E., 2002. Implications of sediment-flux-dependent river incision models for landscape evolution. Journal of Geophysical Research 107 (B2), doi:10.1029/2000JB000044.
Whipple, K.X., Anderson, R., Hancock, G.S., 2000. River incision into bedrock: mechanisms and relative efficacy of plucking, abrasion, and cavitation. Geological Society of America Bulletin 112, 490–503.
Whittaker, J.G., 1987. Sediment transport in step-pool streams. In: Thorne, C.R., Bathurst, J.C., Hey, R.D. (Eds.), Sediment Transport in Gravel-Bed Rivers. Wiley, Chichester, pp. 545–570.
Wilford, G.E., 1991. Exposure of land surfaces, drainage age and erosion rates. In: Ollier, C.D. (Ed.), Ancient Landforms. Belhaven, London, pp. 99–103.
Willet, S.D., 1999. Orogeny and orography: the effects of erosion on the structure of mountain belts. Journal of Geophysical Research 104 (B12), 28,957–28,981.
Williams, G.P., 1983. Paleohydrological methods and some examples from Swedish fluvial environments: I. Cobble and boulder deposits. Geografiska Annaler 65A, 227–243.
Wohl, E.E., 1992a. Bedrock benches and boulder bars: floods in the Burdekin Gorge of Australia. Geological Society of America Bulletin 104, 770–778.
Wohl, E.E., 1992b. Gradient irregularity in the Herbert Gorge of northwestern Australia. Earth Surface Processes and Landforms 17, 69–84.
Wohl, E.E., Merritt, D., 2001. Bedrock channel morphology. Geological Society of America Bulletin 113, 1205–1212.
Wohl, E.E., Greenbaum, N., Schick, A.P., Baker, V.R., 1994. Controls on bedrock channel incision along Nahal Paran, Israel. Earth Surface Processes and Landforms 19, 1–13.
Wolman, M.G., 1954. A method of sampling coarse river bed-material. Transactions-American Geophysical Union 35, 951–956.
Wolman, M.G., Miller, J.P., 1960. Magnitude and frequency of forces in geomorphic processes. Journal of Geology 68, 54–74.